ISSN 1392–1320 MATERIALS SCIENCE (MEDŽIAGOTYRA). Vol. 19, No. 2. 2013

Changes in Storage Properties of Hydrides Induced by Ion Irradiation

Jasmina GRBOVIĆ NOVAKOVIĆ [1] *, Sandra KURKO [1], Željka RAŠKOVIĆ-LOVRE [1], Sanja MILOŠEVIĆ [1], Igor MILANOVIĆ [1], Zoran STOJANOVIĆ [2], Radojka VUJASIN [1], Ljiljana MATOVIĆ [1]

[1] *Vinča Institute of Nuclear Sciences, University of Belgrade P.O.Box 522, 11000 Belgrade, Serbia*
[2] *Institute of Technical Sciences of SASA, Knez Mihailova 35/IV, 11000 Belgrade, Serbia*

crossref http://dx.doi.org/10.5755/j01.ms.19.2.1579

Received 20 April 2012; accepted 13 January 2013

The influence of structural changes caused by irradiation with different ions, their energies and fluences on sorption properties has been investigated. The irradiation has been done using B^{3+} and N^{3+} ions at 45 keV with ion fluence of 10^{16} ion/cm^2 at the FAMA ion source at Vinča Institute of Nuclear Sciences in Belgrade. Morphology and microstructure of samples were analysed using XRD and particle size analysis, while estimation of penetration depth and deposition of defects were done by SRIM calculations. Hydrogen desorption properties and kinetics were evaluated from TPD measurements and numerical non-isothermal procedure. Results suggest that there are several mechanisms of desorption depending on defect concentration, their interaction and ordering. It has been also demonstrated that the changes in near-surface area play the crucial role in hydrogen desorption kinetics. It is confirmed that there is possibility to control the thermodynamic parameters of these systems by controlling vacancies depth profile and concentration.
Keywords: hydrogen storage, MgH_2, ion irradiation, TPD, non- isothermal kinetics.

1. INTRODUCTION

In order to improve MgH_2 storage properties i. e. to decrease the desorption temperature and improve desorption kinetics many efforts have been made [1 – 10]. The concept of metal hydride destabilization (including MgH_2) relies on the capability to identify compounds, elements or methods that can lead to reduction of the reaction enthalpy. This concept is very general and therefore a large number of potential destabilization methods exists [1 – 10]. The commonly used methods are nanostructuring by decrease of particles size to nanometer level by ball milling [1 – 3] and nanostructuring with addition of impurities and/or catalysts [4 – 6]. Both destabilization methods can be declared as bulk modifications since all defects are introduced within whole volume of the sample. Those methods provide some improvements in kinetics and desorption temperature, but the reaction mechanism is still not clear. For example, the rate-limiting step for desorption from MgH_2-Nb_2O_5 composite changes with increasing of milling time or Nb_2O_5 content, from chemisorption to interface velocity of the transformed phase [4]. According to Schulz et al. who investigated MgH_2-V composites, the hydrogen desorption at high temperature and under high driving force, is controlled by the interface (Mg/MgH_2) motion [5]. When the driving force is small, the early stage of hydrogen desorption is controlled by nucleation and growth and the later stage is controlled by long range hydrogen diffusion. At high temperatures, the rate-limiting step changes from interface control (before annealing) to surface control (after annealing), while at low temperatures, the rate-limiting step of desorption does not change after annealing. Therefore, it is quite difficult to understand what actually govern the process especially when one have in mind the fact that the sorption of MgH_2 can be describe by several steps:

(a) Hydrogen in the gas phase transfer to the surface of the metal particle;

(b) Hydrogen diffusion through the boundary layer between gas phase and solid particle;

(c) Physisorption of hydrogen molecules on the solid surface;

(d) Dissociation of hydrogen molecules and chemisorptions;

(f) Surface penetration of hydrogen atoms;

(g) Diffusion of hydrogen atoms through the hydride product layer to the hydride/metal interface and

(h) Chemical reaction and nucleus formation (hydride production)

Any of them could be the rate limiting step [10].

In order to reveal the most important factors governing the sorption properties of MgH_2, it is crucial to obtain a better understanding of the changes induced by the destabilization processes [7 – 11]. We have investigated the influence of well defined structural changes introduced by ion irradiation within surface layer of MgH_2. Understanding of the relations between concentration and type of produced defects and MgH_2 sorption properties will help to overcome some of the material's drawbacks and will provide the possibility to investigate stability of particular induced modifications during desorption.

2. EXPERIMENTAL DETAILS

The commercial (Alfa Aeser) MgH_2 powder was pressed on the Al foil to obtain thin layer and homogeneously irradiated using B^{3+} and N^{3+} ions at 45 keV with ion fluence of 10^{16} ion/cm^2. The irradiation

*Corresponding author. Tel.:+381-11-3408552, fax: +381-11-3408224.
E-mail address: *jasnag@vinca.rs* (J.Grbović Novaković)

was done at FAMA ion source at Vinča Institute. Based on numerical simulations and consequent analysis of depth profile and energy loss mechanisms, 45 keV is found to be an optimal energy to study the near surface effects. The reversibility of the irradiated material wasn't an issue of this study.

Morphological and microanalytical characterization was carried out by VEGA TS 5130MM, Tescan Brno SEM equipped with EDS detector. Malvern 2000SM Mastersizer laser scattering particle size analysis system was used to obtain the quantitative MgH_2 particle size distribution. X-ray diffraction analysis was used to identify the crystalline phases and lattice parameters as well as the crystalline size and strain of irradiated samples by means of Siemens Kristalloflex D-500 device, with Cu-K_α Ni filtrated radiation (λ = 1.5406 Å). Lattice parameters were refined from the fitted data using the least square procedure. Standard deviation obtained was 1 %. Williamson-Hall plots were used to separate the effects of the size and strain in the nanocrystals. Thermal behaviour of the samples was studied by TPD measurements at a constant heating rate of 5 K/min, from room temperature to 973 K, under starting vacuum of 3×10^{-6} mbar, utilizing homemade equipment, with a quadruple mass spectrometer EXTORR XT300. In order to deduce the mechanism of thermal decomposition process [10, 12 – 14] we have used non-isothermal approach under the assumption that the non-isothermal reactions proceed isothermally at an infinitesimal time interval, so that the reaction rate $\frac{d\theta}{dt}$, can be expressed by Arrhenius type equation:

$$\frac{d\theta}{dt} = Ae^{-\frac{E_{des}}{RT}} f(\theta) \ , \tag{1}$$

where A is the pre-exponential factor, θ is degree of conversion, $f(\theta)$ depends on the mechanism of the process involved. Substitution of linear heating rate, β , $\beta = \frac{dT}{dt}$ into Eq. (1) gives:

$$\frac{d\theta}{f(\theta)} = \frac{A}{\beta} e^{-\frac{E^a_{des}}{RT}} dT \ . \tag{2}$$

To evaluate the kinetic parameters from the previous equations, one can plot:

$$\ln\left[\frac{g(\theta)}{T^2}\right] = f\left(\frac{1000}{T}\right). \tag{3}$$

E^a_{des} and A can be calculated from the slope and intercept respectively. Therefore, one can obtain the mechanism by searching for the best fit of the experimental data.

3. RESULTS AND DISSCUSION

3.1. Numerical analysis of irradiation effects

Effects of 45 keV of B^{3+} and N^{3+} ions irradiation of MgH_2 samples are estimated by Monte Carlo simulations with statistics of 10 000 ion events, using the detailed calculation with full damage cascades option of SRIM 2008 code. The main results are presented in Fig. 1, a and b, and Table 1. The B range distribution maximum is found at the depth of 216 nm with the full width at the half of the maximum (FWHM) of 93 nm, indicating a relatively large dispersion of the B^{3+} ions in the samples. A maximum of recoiled Mg and H atoms range is found to be around 167 nm (see Fig. 1, a). Prevalent direct N^{3+} energy loss mechanism is ionization, while direct vacancies production

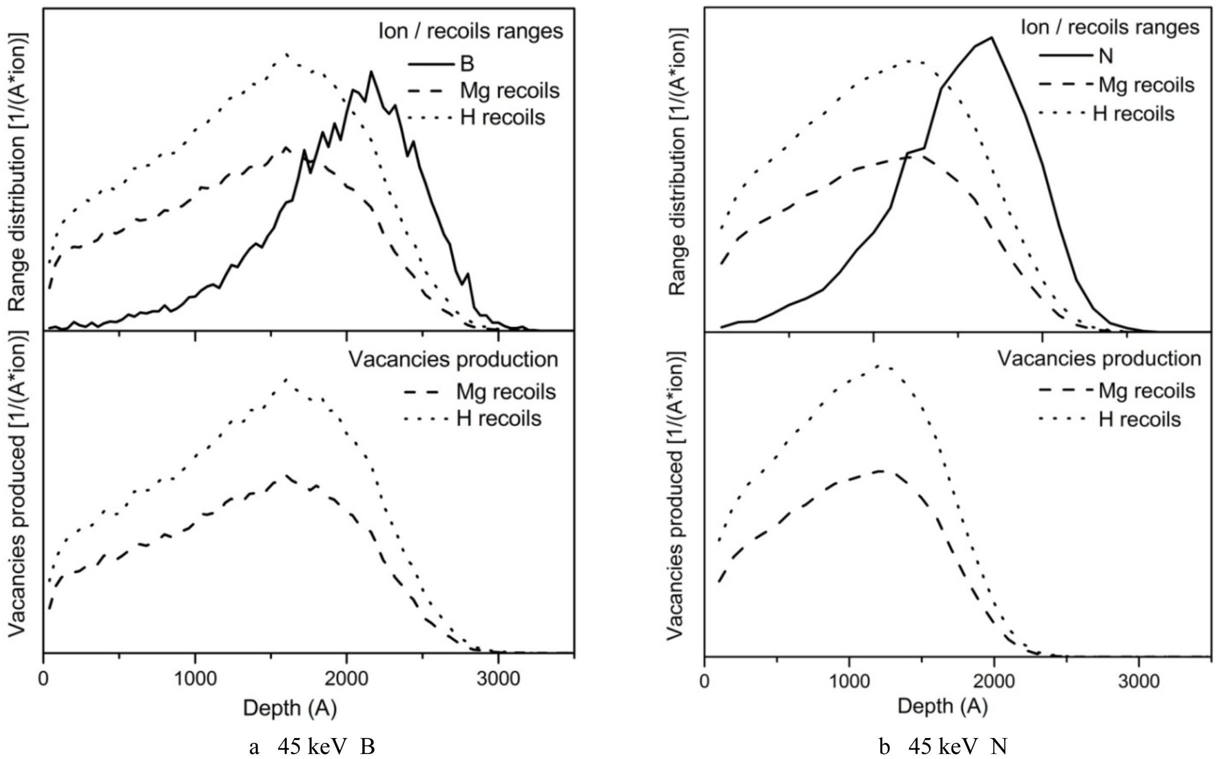

Fig. 1. Monte Carlo simulations of irradiation effects of 45 keV B (a) and N (b) on MgH_2 matrix obtained by SRIM 2003 package: top – depth distribution of incident ions and recoiled atoms; bottom – vacancies production as function of depth

(primary knock-outs) participates with only 0.55 % in total only 1.7 %. The rest of energy is transferred to Mg and H recoils and consecutive cascades with quite different energy loss mechanisms contribution ratio. Similar situation holds for boron irradiation. Recoils loose energy mostly through two competitive processes, ionization and phonon excitation in both cases. The most of incident energy is transferred to recoils (32 % for B compared to 42 % in N case) and consecutive cascades. Further, total number of vacancies per incident B^{3+} ion is found to be 288, which is considerably less than the number of vacancies caused by incident N^{3+} ion of same energy (359 vacancies per ion). Obviously, 45 keV of B^{3+} ions produce less defects, they are placed deeper and spread over a larger distance in the sample, than those produced by corresponding 45 keV N^{3+} irradiation (see Table 1, Fig. 1, b). This is probably the reason for different mechanism and temperature of desorption.

3.2. Morphological and microstructural evaluation of irradiation effects

Sample irradiated with 45 keV of N^{3+} ions (N16) show the morphology quite similar to non treated MgH_2 with agglomerates from 10 μm to 100 μm (Fig. 3, b). Anyhow, figure at higher magnification (Fig. 3, c) shows the typical morphology for irradiated samples i. e. cracks leading to quite damaged onion like structure [7]. On the other hand, agglomerates of sample irradiated with 45 keV of B^{3+} (B16) are much smaller, from 2 μm to 20 μm (Fig. 3, a). This is in agreement with the results of particle size analysis (Fig. 3, Table 2).

Both samples show the monomodal particle size distribution, but with the onset at lower sizes, which is more pronounced for sample irradiated with boron. At first sight, the results of SEM andparticle size analysis seem to be ambiguous, but one should have in mind the fact that particle size analysis was done under constant ultrasound regime since the particles tend toagglomerate.

XRD patterns (Fig. 4) of commercial sample (AA) show narrow peaks at $2\theta = 27.77$ (110), 35.77 (101), 40 (200) 55 (211), characteristic for β-MgH_2 tetragonal structure and minor secondary phase (metallic Mg at $2\theta = 32.35$ and MgO at $2\theta = 36.77$). The irradiated samples exhibit the broadening of typical β-MgH_2 peaks, pointing out a strong influence of ion irradiation on lattice parameters, crystallite size and microstrain (see Table 2).

Table 1. Results of SRIM simulations of 45 keV B^{3+} and N^{3+} ions irradiation of MgH_2 matrix

Species		Range maximum position [nm]	Ion range FWHM [nm]	Vacancies (total per ion)	Energy loss [%]		
					Ionisation	Vacancies production	Phonon exitation
N	Ion	170	90	359	55.58	0.55	1.78
	Recoils	125	159		17.53	1.84	22.72
B	Ion	216	93	288	64.86	0.50	1.80
	Recoils	160	193		13.35	1.41	18.07

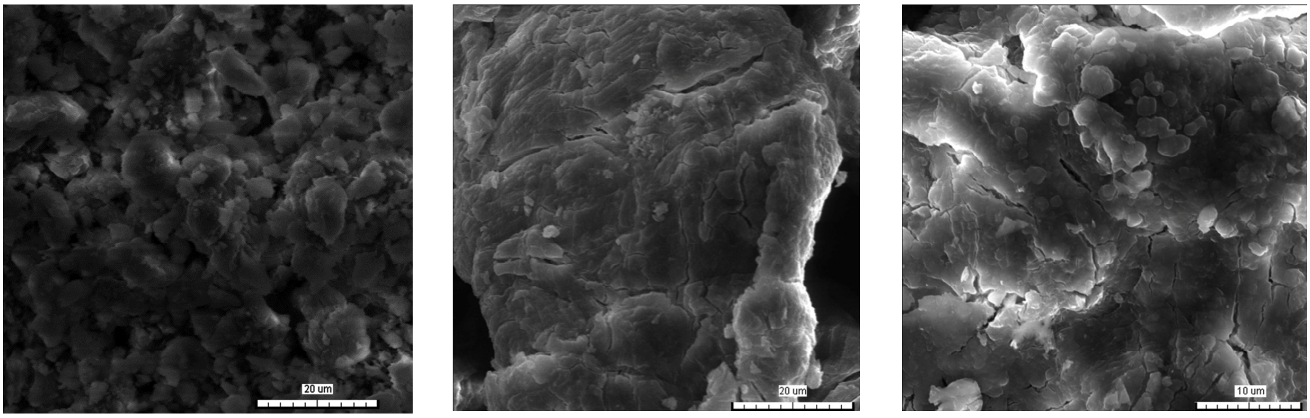

a b c

Fig. 2. SEM micrographs of sample irradiated with 45 keV of B^{3+} (a) and N^{3+} ions (N16) using ion fluence of 10^{16} ion/cm^2 (b) sample N16 marker 20 μm (c) sample N16 marker 10 μm

Table 2. Structural parameters obtained from XRD and particle size analysis of commercial MgH_2 powder (AA) and samples irradiated with 45 keV B^{3+} (B16) and 45 keV N^{3+}(N16) using ion fluence of 10^{16} ion/cm^2

Sample	Crystallite size [nm]	Microstrain	Average particle size [μm]	Lattice parameter of β-MgH_2 [Å]		
				a	*c*	*V*
AA	83	$1.4 \cdot 10^{-3}$	38	4.5168	3.0205	61.623
B16	76	$1.3 \cdot 10^{-3}$	21	4.4915	3.0113	60.744
N16	57	$4.98 \cdot 10^{-4}$	27	4.5132	3.0191	61.498

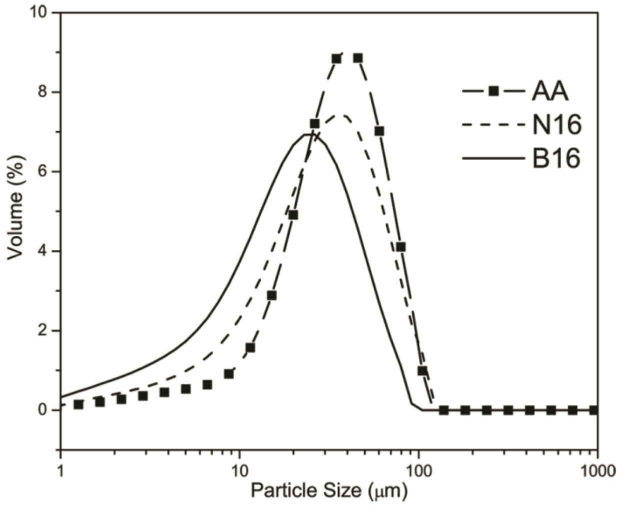

Fig. 3. Particle size analysis of commercial MgH_2 powder (AA) and and samples irradiated with 45 keV B^{3+} (B16) and 45 keV N^{3+}(N16) using ion fluence of 10^{16} ion/cm^2

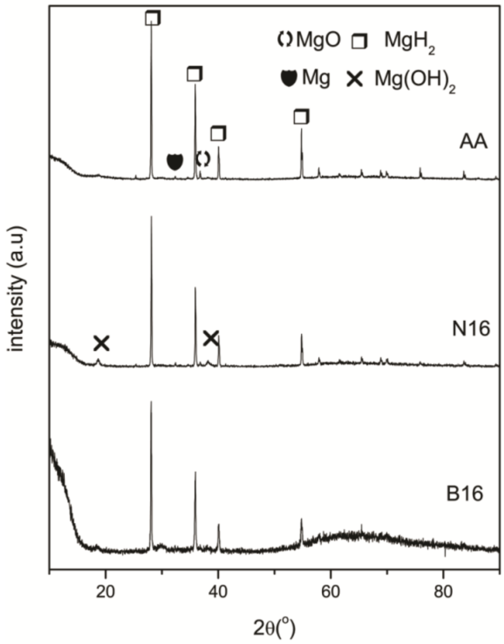

Fig. 4. XRD paterns of commercial MgH_2 powder (AA) and samples irradiated with 45 keV B^{3+} (B16) and 45 keV N^{3+}(N16) using ion fluence of 10^{16} ion/cm^2

In both irradiated samples, some $Mg(OH)_2$ has been formed, but the quantity of hydroxide is much higher in sample were the defects are deposited closer to the surface and where the quantity of defects per incident ion is much higher (sample N16). On the other hand, amorphization is evident in the sample where the defects are positioned deeper into the bulk of sample (sample B16). Further, pronounced decrease of crystallite size is observed for samples irradiated with nitrogen (Table 2). The oxygen contamination during milling process or during XRD or SEM analysis is practically impossible to avoid, even though all experiments has been done under Ar atmosphere.

3.3. Desorption properties and kinetics

Hydrogen desorption properties and kinetics were evaluated from TPD measurements and numerical procedure explained in experimental part (see Fig. 5) [10]. It can be noticed that all the samples completely release hydrogen in a single process. Commercial MgH_2 (AA) releases hydrogen around 710 K while desorption temperature is reduced in both irradiated samples: 661 K for samples irradiated with N^{3+} (N16) and 678 K for sample irradiated with B^{3+} (B16).

The higher temperature of desorption obtained from the samples irradiated with B^{3+} ions, confirm the presumption that both, higher concentration of defects and their distribution closer to the sample surface, enhance the hydrogen desorption rate [8, 10].

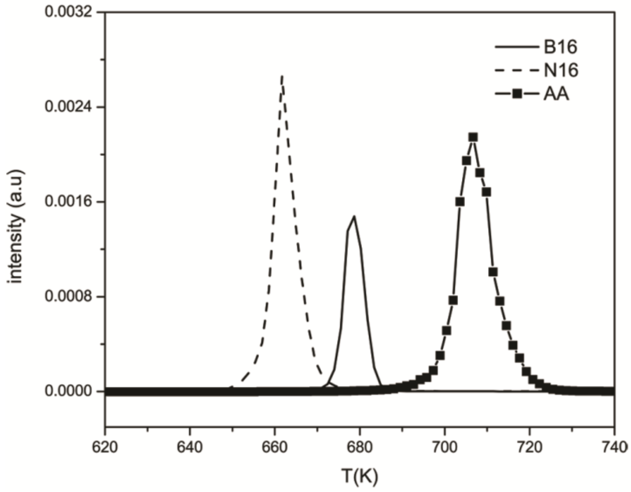

Fig. 5. TPD spectra obtained at heating rate of 5 K/min of commercial MgH_2 sample (AA) and samples irradiated with 45 keV B^{3+} (B16) and 45 keV N^{3+}(N16) using ion fluence of 10^{16} ion/cm^2

The problem of the reaction mechanism is in fact a subject of extensive debate, although grate amount of literature is available [1, 2, 4 – 6, 10 – 20]. Huot et al. suggested that nucleation and growth process takes place during desorption [15]. They found that Avrami parameter in JMA is 3 and interpreted this value as an instantaneous nucleation followed by an interface-controlled three-dimensional growth process. According to Wu et al. [16] the rate-controlling step is the recombination of H_2 on the MgH_2 surface. Leardini et al. indicated that 3D-growth of Mg phase controls the kinetics of MgH_2 decomposition [17]. Ranjbar et al. show that hydrogen desorption reaction for pure MgH_2 is controlled by recombination of chemisorbed hydrogen atoms (surface controlled reaction) [18]. However, upon Ni addition, which is good catalyst for hydrogen molecule dissociation and recombination, the hydrogen desorption reaction is controlled by bulk nucleation and three-dimensional growth of the existing Mg nuclei (JMA 3D) [17]. Liang et al. [19] and Hanada et al. [20], claimed that two-dimensional growth of existing nuclei (JMA 2D) is the rate-limiting step for their Ni doped Mg samples. The results obtained by Barkhordarian et al. indicate that hydrogen diffusion through the dehydrided MgH_2 and through the grain boundaries of the magnesium hydride phase is comparably fast and not rate limiting if Nb_2O_5 is added as catalyst [4]. They have also demonstrated that the rate-limiting step for desorption from MgH_2-Nb_2O_5 composite changes, with increasing of milling time or Nb_2O_5

content, from chemisorption to interface velocity of the transformed phase [4].

On the other hand, controlling the depth of deposition and the number of defects, by ion irradiation, it is possible to unambiguously determine the reaction mechanism. The obtained rate limiting steps of desorption reaction for irradiated material and pure MgH_2 are listed in Table 3. Regarding the untreated sample and B16, the best fit is obtained for phase boundary reaction with spherical symmetry ($n = 3$). On the other hand there is change in kinetics obtained for material irradiated with nitrogen. This fact confirms the presumption that the reaction mechanism depends on quantity and deposition depth of defects.

Table 3. Summary of results obtained after fitting of experimental data (Fig. 6: normalized TPD data)

Sample	Reaction model	Equation	$E_a^{des}\left(\frac{\text{kJ}}{\text{mol}}\right)$
AA	0.3 < θ < 0.9 Avrami Erofeev	$\left[-\ln(1-\theta)\right]^{\frac{1}{3}}$	372
N16	0.3 < θ < 0.9 Avrami Erofeev	$\left[-\ln(1-\theta)\right]^{\frac{1}{4}}$	253
B16	0.3 < θ <0.9 Avrami Erofeev	$\left[-\ln(1-\theta)\right]^{\frac{1}{3}}$	373

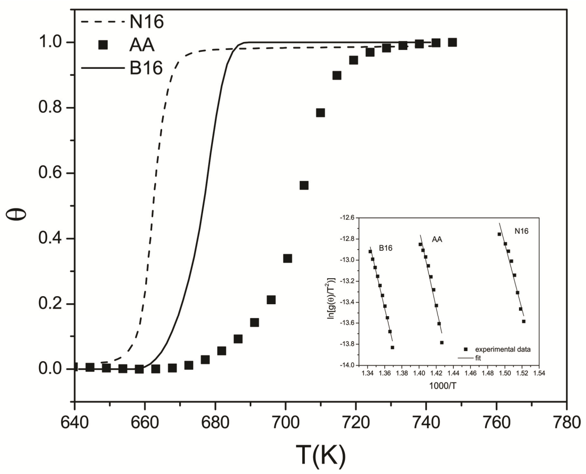

Fig. 6. Temperature evolution of the reacted fraction (θ) corresponding to MgH_2 decomposition, obtained by integration of H_2 peak of commercial MgH_2 (AA), and samples irradiated with 10^{16} ion/cm^2 of 45 keV B^{3+} (B16) and 45 keV N^{3+} (N16) ions

4. CONCLUSION

The influence of structural changes caused by B^{3+} and N^{3+} ion irradiation on sorption properties of MgH_2 has been investigated. The irradiation was done using 45 keV and the fluence of 10^{16} ion/cm^2. Numerical simulations were done in order to obtain the depth profile of incident ions and energy loss mechanisms. Sample irradiated with nitrogen ions show the morphology similar to pure MgH_2 with agglomerates from 10 μm to 100 μm, but with a lot of cracks leading to quite damaged onion like structure. On the other hand, agglomerates of sample irradiated with boron ions are much smaller which is in agreement with the results of particle size analysis. Both samples show the monomodal particle size distribution, but with the onset at lower sizes, which is more pronounced for sample irradiated with boron.

Hydrogen desorption properties and kinetics were evaluated from TPD measurements and numerical non isothermal procedure. Using ion irradiation one can control the depth of deposition and the number of defects, and in such way it is possible to unambiguously explain the change in the reaction mechanism. It has been shown that the reaction mechanism depends on quantity and deposition depth of defects given that the reaction mechanism change from phase boundary reaction with spherical symmetry ($n = 3$) regarding the untreated sample and sample irradiated with boron to phase boundary mechanism with $n = 4$ for sample irradiated with nitrogen. It has been demonstrated that the changes in near-surface area play the crucial role in hydrogen desorption kinetics. It is also confirmed that there is a possibility to control the thermodynamic parameters by controlling vacancies concentration in the investigated systems.

Acknowledgments

This work has been financially supported by the Ministry of Education, Science and Technology under grant III45012.

REFERENCES

1. **Fernandez, J. F., Sanchez, C. R.** Rate Determining Step in the Absorption and Desorption of Hydrogen by Magnesium *Journal of Alloys Compounds* 340 2002: pp. 189 – 198.
2. **Borgschulte, A., Bosenberg, U., Barkhordarian, G., Dornheim, M., Bormann, R.** Enhanced Hydrogen Sorption Kinetics of Magnesium by Destabilized $MgH_{2-\delta}$ *Catalysis Today* 120 (3 – 4) 2007: pp. 262 – 269.
3. **Kurko, S., Rašković, Ž., Novaković, N., Paskaš Mamula, B., Jovanović, Z., Baščarević, Z., Matović, Lj., Grbović Novaković, J.** Hydrogen Storage Properties of MgH_2 Mechanically Milled with α and β *SiC International Journal of Hydrogen Energy* 36 2011: pp. 549 – 554. http://dx.doi.org/10.1016/j.ijhydene.2010.07.022
4. **Barkhordarian, G., Klassen, T., Bormann, R.** Kinetic Investigation of the Effect of Milling Time on the Hydrogen Sorption Reaction of Magnesium Catalyzed with Different Nb_2O_5 Contents *Journal of Alloys and Compounds* 407 2006: pp. 249 – 255. http://dx.doi.org/10.1016/j.jallcom.2005.05.037
5. **Liang, G., Huot, J., Boily, S., Schulz, R.** Hydrogen Desorption Kinetics of a Mechanically Milled MgH_2+5at%V Nanocoposites *Journal of Alloys and Compounds* 305 2000: pp. 239 – 245. http://dx.doi.org/10.1016/S0925-8388(00)00708-8
6. **Du, A. J., Smith, S. C., Lu, G. Q.** First-principle Studies of the Formation and Diffusion of Hydrogen Vacancies in Magnesium Hydride *Journal of Physical Chemistry C* 111 2007: pp. 8360 – 8365.
7. **Grbović Novaković, J., Matović, Lj., Milovanović, S., Drvendžija, M., Novaković, N., Rajnović, D., Šiljegović, M., Kačarević Popović, Z., Ivanović, N.** Changes of Hydrogen Storage Properties of MgH_2 Induced by Heavy Ion Irradiation *International Journal of Hydrogen Energy* 33 2008: pp.1876 – 1879.

8. **Matović, Lj., Novaković, N., Kurko, S., Šiljegović, M., Matović, B., Kačarević Popović, Z., Romčević, N., Ivanović, N., Grbović Novaković, J.** Structural Destabilisation of MgH_2 Obtained by Heavy Ion Irradiation *International Journal of Hydrogen Energy* 34 2009: pp. 7275 – 7282.

9. **Kurko, S., Matović, Lj., Novaković, N., Matović, B., Jovanović, Z., Paskaš Mamula, B., Grbović Novaković, J.** Changes of Hydrogen Storage Properties of MgH_2 Induced by Boron Ion Irradiation *International Journal of Hydrogen Energy* 36 (1) 2011: pp.549 – 554.

10. **Matović, Lj., Kurko, S., Rašković-Lovre, Ž., Vujasin, R., Milanović, I., Milošević, S., Grbović Novaković, J.** Assessment of Changes in Desorption Mechanism of MgH_2 after Ion Bombardment Induced Destabilization *International Journal of Hydrogen Energy* 37 (8) 2012: pp. 6727 – 6732. http://dx.doi.org/10.1016/j.ijhydene.2012.01.084

11. **Gulicovski, J., Raskovic-Lovre, Z., Kurko, S., Vujasin, R., Jovanovic, Z. Matovic, Lj., Grbovic Novakovic, J.** Influence of Vacant CeO_2 Nanostructured Ceramics on MgH_2 Hydrogen Desorption Properties *Ceramics International* 38 2012: pp. 1181 – 1186. http://dx.doi.org/10.1016/j.ceramint.2011.08.047

12. **Avrami, M.** Kinetics of Phase Change. I: General Theory *Journal of Chemical Physics* 7 1939: pp. 1103 – 1012.

13. **Mintz, M. H., Zeiri, Y.** Hydriding Kinetics of Powders *Journal of Alloys and Compounds* 216 1994: pp. 159 – 175. http://dx.doi.org/10.1016/0925-8388(94)01269-N

14. **Sestak, J., Berggren, G.** Study of the Kinetics of the Mechanism of Solid-state Reactions at Increasing Temperature *Thermochimica Acta* 3 1971: pp.1 – 12.

15. **Huot, J., Liang, G., Boily, S., Van Neste, A., Schulz, R.** Structural Study and Hydrogen Sorption Kinetics of Ball-milled Magnesium Hydride *Journal of Alloys and Compounds* 293 – 295 1999: pp. 495 – 500.

16. **Wu, G., Zhang, J., Li, Q., Wu, Y., Chou, K. C., Bao, X.** Dehydrogenation Kinetics of Magnesium Hydride Investigated by DFT and Experiment *Computational Materials Science* 49 2010: pp. S144 – 149. http://dx.doi.org/10.1016/j.commatsci.2010.02.048

17. **Leardini, F., Ares, J. R., Bodega, J., Fernandez, J. F., Ferrer, I. J., Sanchez, C.** Reaction Pathways for Hydrogen Desorption from Magnesium Hydride/hydroxide Composites: Bulk and Interface Effects *Physical Chemistry Chemical Physics* 12 2010: pp. 572 – 577. http://dx.doi.org/10.1039/b912964b

18. **Ranjbar, A., Guo, Z. P., Yu, X. B., Attard, D., Calka, A., Liu, H. K.** Effects of SiC Nanoparticles with and without Ni on the Hydrogenstorage Properties of MgH_2 *International Journal of Hydrogen Energy* 34 2009: pp. 263 – 7268. http://dx.doi.org/10.1016/j.ijhydene.2009.07.005

19. **Liang, G., Huot, J., Boily, S., Neste, A. V.** Catalytic Effect of Transition Metals on Hydrogen Sorption Innanocrystal-line Ball Milled MgH_2-Tm (Tm = Ti, V, Mn, Fe and Ni) Systems *Journal of Alloys and Compounds* 292 1999: pp. 247 – 252. http://dx.doi.org/10.1016/S0925-8388(99)00442-9

20. **Hanada, N., Ichikawa, T., Fujii, H.** Catalytic Effect of Nanoparticle 3D-transition Metals on Hydrogen Storage Properties in Magnesium Hydride MgH_2 Prepared by Mechanical Milling *Journal of Physical Chemistry B* 109 2005: pp. 7188 – 7194.